doi:10.2533/chimia.2007.179 CHIMIA **2007**, *61*, No. 4

Chimia 61 (2007) 179–183

ISSN 0009–4293

Light-Induced Spin Crossover Probed by Ultrafast Optical and X-ray Spectroscopies

Wojciech Gawelda[§a,b], Andrea Cannizzo[a], Van-Thai Pham[a], Amal El Nahhas[a], Christopher J. Milne[a], Renske van der Veen[a], Christian Bressler[a], and Majed Chergui*[a]
[§]SCS Poster Prize Winner

Abstract: The photoinduced energy and structural relaxation of aqueous iron(II)-tris-bipyridine ($[Fe^{II}(bpy)_3]^{2+}$), upon excitation into its singlet metal-to-ligand charge transfer (^{1}MLCT) band, and the population of its short-lived (≤0.6 ns) high-spin excited state have been characterized by combined ultrafast optical and X-ray spectroscopies. Polychromatic femtosecond fluorescence up-conversion reveals a very short lived ^{1}MLCT emission band, which decays in ≤20 fs by intersystem crossing to a ^{3}MLCT, whose very weak emission is also observed. Transient absorption studies show that the latter decays in <150 fs, while the population of the lowest excited high spin quintet state $^5T_2$ occurs in ~1 ps. Subsequently it decays in ~665 ps to the ground state. Therefore, we determined the structure of the high-spin excited state by picosecond X-ray absorption spectroscopy at the *K* edge of Fe. The structural analysis of both the transient difference and excited state X-ray spectra delivered an Fe–N bond elongation of 0.2 Å in the quintet state compared to the singlet ground state.

Keywords: Fluorescence · Iron (II) complexes · Optical absorption · Spin crossover · Ultrafast · X-ray Absorption

1. Introduction

Ferrous molecular complexes have been intensively studied due to their interesting electronic and magnetic properties, particularly in relation to the phenomenon of spin crossover (SCO), which implies an electron spin flip between a low spin (LS) ground state and a high spin (HS) excited state. This process can be triggered by either temperature or light,[1] while the reverse transition can also be induced by pressure.[2] The study of SCO compounds has been additionally motivated by their potential applications in magnetic data storage[3] and as bistable molecular devices,[4] where the ultrafast spin changes offer a novel route for even faster data processing at the molecular scale.[5]

*Correspondence: Prof. Dr. M. Chergui[a]
Tel.: +41 21 693 3055
Fax: + 41 21 693 3042
E-Mail: Majed.Chergui@epfl.ch
[a]Ecole Polytechnique Fédérale de Lausanne
Laboratoire de Spectroscopie Ultrarapide
Institut des Sciences et Ingénierie Chimiques
FSB-BSP, ISIC, LSU
CH-1015 Lausanne
[b]Paul Scherrer Institut
Swiss Light Source
CH-5232 Villigen

Iron(II)-tris-bipyridine, $[Fe^{II}(bpy)_3]^{2+}$, represents a typical LS compound, whose characteristic energy level scheme is shown in Fig. 1. Contrary to most SCO compounds, in $[Fe^{II}(bpy)_3]^{2+}$ the spin transition can only be optically triggered, while the HS state can be stabilized at cryogenic temperatures, in the so-called light-induced excited spin state trapping (LIESST) process.[1,6] Most SCO complexes, including $[Fe^{II}(bpy)_3]^{2+}$, are characterized by an intense broad band centered at ~520 nm, due to the ^{1}MLCT states (Fig. 1). Excitation by UV-Vis light populates the latter and is followed by a relaxation cascade, presumably through a manifold of singlet, triplet and quintet MLCT and ligand-field (LF, also called metal-centered, MC, states), which brings the system to the lowest-lying excited quintet state, $^5T_2$, with almost unit quantum yield.[7,8]

The kinetics of light-induced SCO have been characterized by conventional and ultrafast laser techniques over the past few years.[6,8–12] These studies indirectly inferred that the relaxation from the initially excited ^{1}MLCT state to the lowest $^5T_2$ quintet state occurs within <1 ps. Subsequently, the quintet state relaxes non-radiatively to the LS ground state in ~0.65 ns in aqueous solution at room temperature, as determined in ground-state bleach recovery experiments.[10] However, the details of the intermediate steps going from the initially accessed ^{1}MLCT state to the $^5T_2$ state have not been clearly resolved, and it was previously suggested that the population of the $^5T_2$ state is directly fed from the ^{1}MLCT excitation.[9,11] The quintet state is characterized by redistribution of the 3*d* electrons into antibonding e_g orbitals, which should

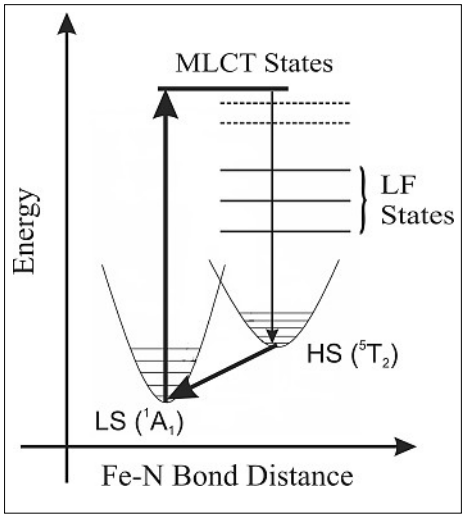

Fig. 1. Energy level scheme of $[Fe^{II}(bpy)_3]^{2+}$ displaying both the low-spin (LS) ground state $^1A_1$ and the lowest-lying excited high-spin (HS) state $^5T_2$, together with the intermediate metal-to-ligand charge transfer (MLCT) and ligand-field (LF) states

therefore lead to an elongation of the Fe–N bond. In Fe(II) complexes, with long-lived quintet states (up to days[6,13]), the Fe–N bond elongation was determined using static X-ray techniques and LIESST, to lie around 0.2 Å.[14–19] The same was predicted from *ab initio* calculations for $[Fe^{II}(bpy)_3]^{2+}$,[20] implying a significant structural change during the relaxation cascade of ~1 ps, from the ^{1}MLCT to the lowest quintet state.

In order to elucidate the intermediate steps from the ^{1}MLCT to the $^5T_2$ state and their timescale, and to determine the structure of the quintet state, we have used a combination of femtosecond fluorescence up-conversion, femtosecond transient absorption (TA) and picosecond X-ray absorption spectroscopy. This combination of methods allows us to fully map out the details of the relaxation cascade within the first picosecond and beyond, and to determine the transient molecular structure of the HS species at room temperature and in 'real-time'.

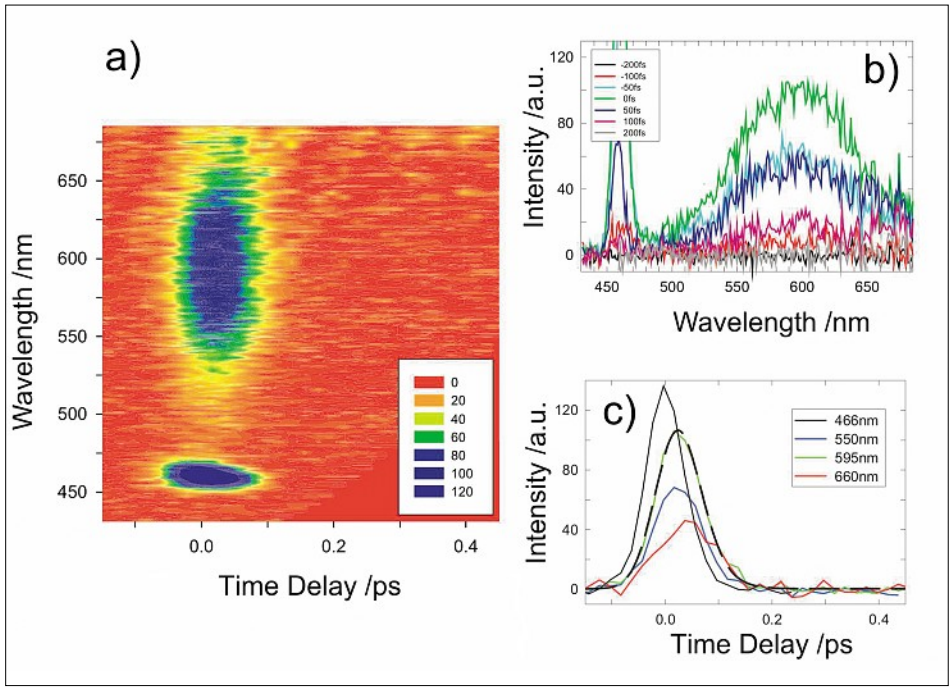

Fig. 2. a) Two-dimensional plot of the femtosecond fluorescence spectra of an aqueous $[Fe^{II}(bpy)_3]^{2+}$ under excitation at 400 nm. The signal at 466 nm is the Raman line of H_2O. b) Fluorescence spectra at different time delays. c) Time traces at different wavelengths. Time delays are taken with respect to the water Raman line (466 nm, not shown here). The trace at 595 nm is shown together with its fit function.

2. Experimental

The details of the experimental setup and the data acquisition strategy are described elsewhere.[21–25] Briefly, for the fluorescence measurements, we performed the experiments in the 440–690 nm detection range, with a resolution of 110±10 fs. The sample is excited at 400 nm with pulses of *ca.* 100 fs. The fluorescence signal, collected in a forward scattering geometry, was up-frequency converted in a 250 µm thick BBO crystal by mixing with a pulse at 800 nm (the so-called gate pulse). The up-converted signal is spatially filtered and detected in polychromatic mode with a spectrograph and a liquid N_2-cooled CCD camera.

For the TA measurements, we use 150 fs pulses at 400 nm for excitation. Probing is done using a broadband white light continuum in the UV-Vis, which is dispersed after the sample in a spectrometer and detected by a double diode array, allowing the recording of transmission between 350 and 650 nm. The probe beam was detected at the nominal repetition rate of the laser (1 kHz), so that the adjacent pairs of pumped and unpumped spectra are obtained delivering, after subtraction, the transient spectra.

The laser-pump/X-ray-probe experiments were performed at the microXAS beamline of the Swiss Light Source (SLS). Pumping the system is achieved by 150 fs, 400 nm laser pulses, while probing is done by monochromatic and tunable hard X-ray pulse (probe pulse) of 75 ps temporal width, which is spatially overlapped with the laser pump pulse onto the sample. The photoinduced changes are monitored during the experiment as a function of the adjustable pump-probe time delay Δt. The detected signal is the difference X-ray absorption spectrum (recorded in both X-ray transmission and fluorescence modes) between the laser excited and the unexcited sample, recorded on a shot-to-shot basis at twice the repetition rate of the laser pump pulse. In all the above experiments, the sample was a free-flowing liquid jet of an aqueous solution of 1–25 mM $[Fe^{II}(bpy)_3]^{2+}$.

3. Results and Discussion

3.1. *Femtosecond Fluorescence Spectroscopy*

Fig. 2a shows a typical 2D fluorescence spectrum obtained upon excitation of an aqueous $[Fe^{II}(bpy)_3]^{2+}$ at 400 nm. The time-dependent emission spectra, which are shown in Fig. 2b, are obtained by taking slices at fixed time delay, while cuts at fixed emission wavelength provide the kinetic traces, shown in Fig. 2c. Strikingly, the emission shows up in the 500–650 nm region already at t = 0 and is very short lived, *i.e* in the order of the instrument temporal response. In addition, in Fig. 2a, a weak emission shows up at $\lambda \geq 650$ nm and $t \geq 100$ fs. This observation is confirmed in Fig. 2b, where the spectrum at t = 100 fs exhibits two weak bands of almost identical intensity, one centered at ~600 nm, the other at ~660 nm. The former is the remnant of the main emission at earlier times.

We also verified that no other emissions occur at longer times, by recording scans up to 250 ps time delay. The comparison of Raman and emission time traces (Fig. 2c) suggests a rise and a decay of the fluorescence almost within the cross-correlation of our experiment for all kinetic traces at <650 nm. These results bear some analogy with those of $[Ru^{II}(bpy)_3]^{2+}$.[21] Indeed, the 600 nm centered emission in Fig. 2a is Stokes-shifted with respect to the ^{1}MLCT absorption by ~2600 cm^{-1}, as compared to ~3000 cm^{-1} for $[Ru^{II}(bpy)_3]^{2+}$. Furthermore, kinetic traces at <650 nm in Fig. 2c are best fitted with an exponential decay of 20±5 fs convoluted with the instrumental response, which again is similar to the case of Ru complex.[21] Based on these analogies, we attribute the main emission at ~600 nm to the ^{1}MLCT state, while the weak band at ~660 nm is assigned to the ^{3}MLCT state. The latter assignment is based on the fact that, just as in $[Ru^{II}(bpy)_3]^{2+}$, the ^{1}MLCT decays to the ^{3}MLCT on similar very short timescales.

3.2. *Femtosecond Optical Absorption Spectroscopy*

Fig. 3a shows representative spectra recorded at various time delays within the initial 2 ps after photoexcitation. A short-lived excited state absorption (positive signal) appears in the 340–440 nm region, while in the 560–640 nm range, it is present even at longer time delays. In <200 fs, the short wavelength (<400 nm) excited state absorption is replaced by a negative signal, which we identify as the ground state bleach (GSB) signal, caused by depletion

of the ground state due to the photoexcitation by the pump pulse. This bleach signal is dominant in the 450–550 nm spectral range and it fully reflects the ground state absorption. It is interesting to note that the short lived excited state absorption (ESA) at <400 nm, is identical to what we found in $[Ru^{II}(bpy)_3]^{2+}$,[26] which we attributed to the ^{3}MLCT absorption. Kinetic traces at three characteristic wavelengths (370 nm, 523 nm and 630 nm) are shown in Fig. 3b. It can be seen that the positive absorption signals at 370 and 630 nm appear within the experimental temporal resolution of 140 fs, but behave differently, as already noted in Fig. 3a. In particular, the 630 nm trace shows the same rapid rise as the 370 nm trace, but the subsequent kinetics is completely different.

We used singular value decomposition and a global fit analysis to analyze the spectral and kinetic traces together. The details of the procedure and the results are given in ref.[22] Here we assumed a kinetic scheme where the relaxation proceeds by sequential steps. Our model globally delivered three time constants: 115±10 fs, 960±100 fs and 665±35 ps that fitted simultaneously all the kinetic traces in the spectral range of interest. In addition, we obtained the so-called decay-associated spectra (DAS), not shown here, corresponding to the three decay components (Fig. 3b). The DAS associated with the shortest component confirms that it is the reduced form of $[Fe^{II}(bpy)_3]^{2+}$ complex, which results from excitation to the MLCT states. The longest component has, as expected, a DAS that reflects the ground state absorption spectrum and is associated with the decay of the $^5T_2$ state and the population of the $^1A_1$ ground state. Finally, the DAS of the intermediate component cannot be associated to any given photochemical species in a straightforward way, as it contains contributions from several states in the relaxation cascade (Fig. 1). We attribute the time constant of 960 fs to the population (arrival) time of the excited $^5T_2$ state, in agreement with the previously estimated singlet to quintet relaxation time.[11] Because the ^{3}MLCT state is populated in ≤20 fs from the ^{1}MLCT state and it decays in ~100 fs according to the fluorescence data (Fig. 2a), we associate the 115±10 fs component to the departure from the ^{3}MLCT state.

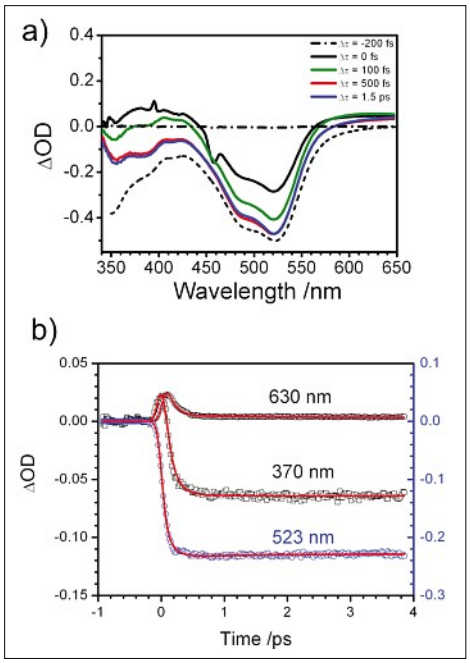

Fig. 3. a) Transient absorption spectra of aqueous $[Fe^{II}(bpy)_3]^{2+}$ upon 400 nm excitation. The spectral evolution in the first 1.5 ps after photoexcitation (t = 0) is shown. The peak around 400 nm at t = 0 is the residual scattered light contribution from the pump pulse. The strong negative absorption feature present in the early spectra around 450–460 nm is the impulsively-induced Raman signal of H_2O. The inverted ground state absorption spectrum is displayed (dashed line) for comparison. b) Kinetic traces of aqueous $[Fe^{II}(bpy)_3]^{2+}$ in a 5 ps time window at three selected wavelengths, together with their fit functions using a global fit model (see text for further details).

In summary, the ultrafast fluorescence and transient absorption studies have allowed us to unravel several hitherto unobserved steps of the relaxation sequence, which are summarized in Fig. 4:

i) The ultrafast ^{1}MLCT→^{3}MLCT intersystem crossing.
ii) The departure from the ^{3}MLCT.
These two results establish the ^{3}MLCT as an intermediate in the relaxation cascade.
iii) The arrival time in the $^5T_2$ state in ~1 ps.
iv) The decay of the $^5T_2$ state, which we detect by monitoring the excited state absorption at λ >620 nm. It governs the re-population of the ground $^1A_1$ state.

3.3. *Picosecond X-ray Absorption Spectroscopy*

The unit quantum efficiency for population of the $^5T_2$ state,[7] its rise time of 1 ps and decay of 665 ps, imply that this state is a bottleneck to population relaxation. Therefore, all excited molecules ultimately reach the $^5T_2$ state in ≤1 ps, and hence its structure can be detected by time-resolved X-ray absorption spectroscopy with our current temporal resolution of 70 ps.[27]

Fig. 5a shows the static K-edge X-ray absorpion (XAS) spectrum of a 25 mM aqueous $[Fe^{II}(bpy)_3]^{2+}$ complex. It is characterized by a number of X-ray near-edge structure (XANES) features, which are displayed in the inset figure, that have already been discussed for similar ferrous molecular complexes.[28,29] The features that lie ≥50 eV above the edge are above-ionization features dominated by scattering from the nearby N-atoms, in particular feature

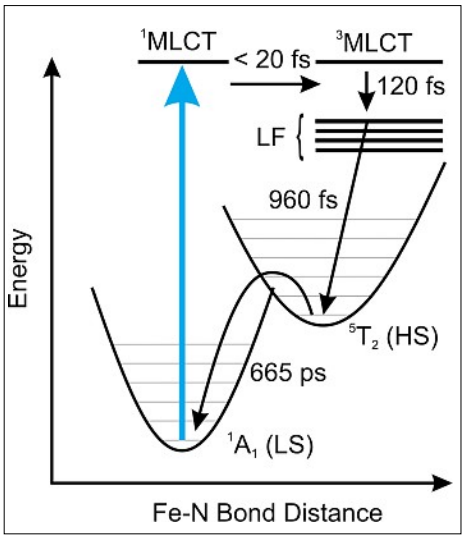

Fig. 4. Photochemical cycle of room-temperature aqueous $[Fe^{II}(bpy)_3]^{2+}$. The characteristic lifetimes obtained in the present study are displayed and the inclusion of ^{3}MLCT in the relaxation cascade is established. The horizontal blue arrow indicates the single photon excitation energy of 3.1 eV (400 nm).

E. The exact assignment of the XANES features will not be discussed here, but all have been shown to undergo significant changes upon spin transition in static XAS studies,[15,16,28,29] in particular bands B–E. Most of these changes have been attributed to changes of metal–ligand and intraligand bond distances and angles, with the Fe–N bond being the dominant contributor. Additional changes in the high energy (EXAFS) region were also clearly observed, which likewise point to a significant Fe–N bond change.

Fig. 5b shows the transient difference spectrum measured 50 ps after laser excitation. All the above-mentioned changes are indeed occurring as a result of laser excitation and transient population of the $^5T_2$ state. That the latter is responsible for these changes is confirmed by the inset in Fig. 5b, which compares the temporal evolution of the absorption changes at the B-feature (7126 eV) with the kinetics of the ground state recovery measured by femtosecond optical pump-probe spectroscopy. The latter reflects the repopulation of the LS state by the decay of the HS state and it matches the X-ray data perfectly. The difference absorption spectrum in Fig. 5b is defined as:[30]

$$T(E,t) = f(t).[A_{HS}(E,t) - A_{LS}(E)] \quad (1)$$

where $f(t)$ is the fractional population of the HS complex at time t (50 ps in Fig. 5b), $A_{LS}(E)$ is the absorption spectrum of the LS complex (Fig. 5a), and $A_{HS}(E,t)$ that of the HS complex, at time t following the photoexcitation. In order to extract the excited state structure correctly, $f(t)$ must be known, and we measured a value of 22(2)%

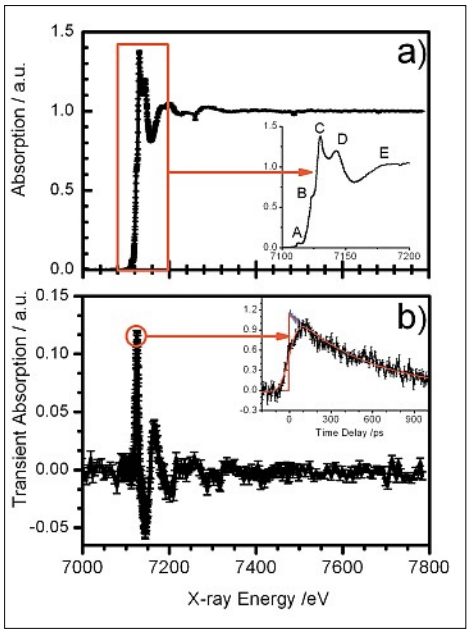

Fig. 5. a) *K*-edge X-ray absorption spectrum of the ground LS state of aqueous $[Fe^{II}(bpy)_3]^{2+}$. The inset zooms into the first 100 eV of the spectrum and displays the details of the absorption edge and the nearest-lying XANES resonances (labeled from A–D). The onset of the EXAFS range is represented by the E feature. b) Transient difference spectrum, recorded 50 ps after the laser pump pulse, with its error bars. The inset displays the kinetics traces of the transient X-ray absorption signal recorded at 7126 eV (feature A) as compared to the optical signal (blue) recorded in transmission at 523 nm. The rise time of the X-ray signal is determined by the 70 ps width of the X-ray probe pulse.

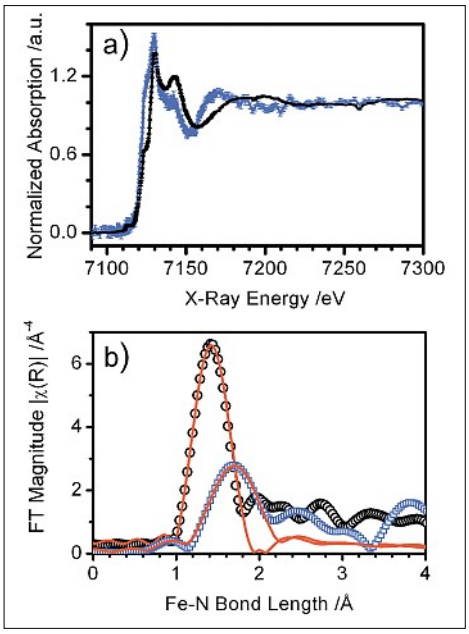

Fig. 6. a) XAS spectra of the LS (black) and HS (blue) states of a 25 mM aqueous solution of $[Fe^{II}(bpy)_3]^{2+}$. b) The Fourier power spectra of k^3-weighted EXAFS spectra of the LS (circles) and HS (squares) complexes together with their fits (solid lines) using a first-shell model with six nearest neighbour N atoms.

at t = 50 ps, in laser-only pump-probe experiments.[31]

The results presented in Fig. 5 form the input of the structural analysis, which was initiated by extracting the excited HS state spectrum, with the help of Eqn. (1) and the value of $f(t = 50$ ps). In Fig. 6a, we compare the LS (black) and HS (blue) spectra of the aqueous $[Fe^{II}(bpy)_3]$. We note that all photoinduced spectral modulation captured by the transient difference XAS spectrum from Fig. 5b are now present in the excited state spectrum and are properly weighted according to $f(t = 50$ ps) (see Eqn. (1)). Finally, the spectra from Fig. 6a have been used in the quantitative structural analysis, were fits of the k^3-weighted EXAFS spectra of both spin states of $[Fe^{II}(bpy)_3]^{2+}$ have been carried out using the scattering amplitudes and phases obtained with the FEFF 8.20 code.[32]

Fig. 6b shows a comparison of the Fourier-transformed experimental and fitted spectra (not corrected for the central atom phase shift, which corresponds to *ca.* 0.3 Å). The fits were obtained using the first-shell nitrogen contribution only and both LS and HS Fe–N bond distances were freely optimized in the fits (restrained to all six N atoms having the same bond distance in a nearly octahedral arrangement). The LS bond distance is 1.99±0.02 Å, while for the HS state we find R_{HS} = 2.19±0.04 Å, which as a first experimental measurement of this entity, is in a very good agreement with previous quantum chemical predictions obtained by DFT calculations[20] and experimental results for similar ferrous spin crossover complexes measured either by time-resolved[33] or static[14–16] structure-sensitive methods.

4. Conclusions

In this investigation of the relaxation cascade in aqueous solution of $[Fe^{II}(bpy)_3]^{2+}$ complex we have unraveled a number of processes which are operative in other coordination chemistry compounds:

The initial step is identified as an ultrafast intersystem crossing from the ^{1}MLCT to the ^{3}MLCT in ≤20 fs. This anomalously high relaxation rate is identical in $[Ru^{II}(bpy)_3]^{2+}$, and is therefore independent of the spin-orbit constant of the metal atom. This process is mediated by the high frequency modes of the molecule and is therefore a strongly non-adiabatic process.

We identify the relaxation from the ^{3}MLCT in ~120 fs and the arrival in the $^5T_2$ state in ~1 ps. The whole cascade, starting from the ^{1}MLCT to the $^5T_2$ state, corresponds to an overall energy dissipation of 2000 cm^{-1}/100 fs, given the entire process takes place in less than 1 ps. Although these are high rates they do not occur in a non-Born-Oppenheimer regime contrary to the initial ISC step.[31]

We have determined the structure of the $^5T_2$ HS excited state of $[Fe^{II}(bpy)_3]^{2+}$, and derived an Fe–N bond elongation $\Delta R_{HL} \equiv R_{HS}–R_{LS}$ = 0.2±0.04 Å.[27] Interestingly, this elongation is nearly identical for all complexes, despite their largely different HS lifetimes. This confirms that the driving force for the HS→LS relaxation is mainly determined by the energetics of the HS state, rather than its geometry.[34]

In summary, using a combination of ultrafast optical and X-ray techniques we have captured the transient energetics and the structural rearrangements, allowing us to complete the picture of the involved relaxation intermediates following from the singlet ^{1}MLCT to the HS state. However, several intermediate steps occurring in ≤1 ps cannot easily be resolved by optical probes, as they involve spectroscopically silent states. With the advent of sources delivering tunable femtosecond X-ray pulses,[35] it will eventually become possible to capture these intermediates by ultrafast X-ray absorption spectroscopy.

Acknowledgements

This work was funded by the Swiss National Science Foundation (FNRS), through Contracts No. 620-066145, No. 200021-107956, and No. 200021-105239. We thank Drs Maik Kaiser, Steven Johnson, Daniel Grolimund, Paul Beaud, Gerhard Ingold and Rafael Abela for their support and assistance in the X-ray experiments at the Swiss Light Source (Paul Scherrer Institut, Villigen).

Received: December 18, 2006

[1] P. Gutlich, A. Hauser, H. Spiering, *Angew. Chem., Int. Ed.* **1994**, *33*, 2024.
[2] V. Ksenofontov, A. B. Gaspar, P. Gutlich, *Top. Curr. Chem.* **2004**, *235*, 23.
[3] J. F. Letard, P. Guionneau, L. Goux-Capes, *Top. Curr. Chem.* **2004**, *235*, 221.
[4] Y. Garcia, J. Moscovici, A. Michalowicz, V. Ksenofontov, G. Levchenko, G. Bravic, D. Chasseau, P. Gutlich, *Chem.-Eur. J.* **2002**, *8*, 4992.
[5] G. P. Zhang, W. Hubner, E. Beaurepaire, J. Y. Bigot, *Top. Appl. Phys.* **2002**, *83*, 245.
[6] A. Hauser, *Top. Curr. Chem.* **2004**, *234*, 155.
[7] M. A. Bergkamp, C. K. Chang, T. L. Netzel, *J. Phys. Chem.* **1983**, *87*, 4441.
[8] C. Brady, J. J. McGarvey, J. K. McCusker, H. Toftlund, D. N. Hendrickson, *Top. Curr. Chem.* **2004**, *235*, 1.
[9] E. A. Juban, A. L. Smeigh, J. E. Monat, J. K. McCusker, *Coord. Chem. Rev.* **2006**, *250*, 1783.
[10] J. K. McCusker, K. N. Walda, R. C. Dunn, J. D. Simon, D. Magde, D. N. Hendrickson, *J. Am. Chem. Soc.* **1992**, *114*, 6919.

[11] J. K. McCusker, K. N. Walda, R. C. Dunn, J. D. Simon, D. Magde, D. N. Hendrickson, *J. Am. Chem. Soc*. **1993**, *115*, 298.
[12] J. E. Monat, J. K. McCusker, *J. Am. Chem. Soc.* **2000**, *122*, 4092.
[13] A. Hauser, C. Enachescu, M. L. Daku, A. Vargas, N. Amstutz, *Coord. Chem. Rev*. **2006**, *250*, 1642.
[14] P. Guionneau, M. Marchivie, G. Bravic, J. F. Letard, D. Chasseau, *Top. Curr. Chem*. **2004**, *234*, 97.
[15] H. Oyanagi, T. Tayagaki, K. Tanaka, *J. Phys. Chem. Solids* **2004**, *65*, 1485.
[16] H. Oyanagi, T. Tayagaki, K. Tanaka, *J. Lumin.* **2006**, *119*, 361.
[17] M. Hostettler, K. W. Tornroos, D. Chernyshov, B. Vangdal, H. B. Burgi, *Angew. Chem., Int. Ed*. **2004**, *43*, 4589.
[18] J. Kusz, D. Schollmeyer, H. Spiering, P. Gutlich, *J. Appl. Cryst.* **2005**, *38*, 528.
[19] T. Yokoyama, Y. Murakami, M. Kiguchi, T. Komatsu, N. Kojima, *Phys. Rev. B* **1998**, *58*, 14238.
[20] L. M. L. Daku, A. Vargas, A. Hauser, A. Fouqueau, M. E. Casida, *ChemPhysChem* **2005**, *6*, 1393.
[21] A. Cannizzo, F. van Mourik, W. Gawelda, G. Zgrablic, C. Bressler, M. Chergui, *Angew. Chem., Int. Ed.* **2006**, *45*, 3174.
[22] W. Gawelda, 'Time-Resolved X-ray Absorption Spectroscopy of Transtion Metal Complexes', Ph.D. Thesis, EPFL, Lausanne, **2006**.
[23] G. Zgrablic, 'Solvent Effects on the Ultrafast Dynamics of the Retinal Chromophore of Bacteriorhodopsin', Ph.D. Thesis, EPFL, Lausanne, **2006**.
[24] W. Gawelda, C. Bressler, M. Saes, M. Kaiser, A. Tarnovsky, D. Grolimund, S. L. Johnson, R. Abela, M. Chergui, *Physica Scripta* **2005**, *T115*, 102.
[25] M. Saes, F. van Mourik, W. Gawelda, M. Kaiser, M. Chergui, C. Bressler, D. Grolimund, R. Abela, T. E. Glover, P. A. Heimann, R. W. Schoenlein, S. L. Johnson, A. M. Lindenberg, R. W. Falcone, *Rev. Sci. Instrum*. **2004**, *75*, 24.
[26] A. Tarnovsky, W. Gawelda, M. Johnson, C. Bressler, M. Chergui, *J. Phys. Chem. B* **2006**, *110*, 26497.
[27] W. Gawelda, V.-T. Pham, M. Benfatto, Y. Zaushitsyn, M. Kaiser, D. Grolimund, S. L. Johnson, R. Abela, A. Hauser, C. Bressler, M. Chergui, *Phys. Rev. Lett*. **2007**, *98*, 057401.
[28] V. Briois, C. C. D. Moulin, P. Sainctavit, C. Brouder, A. M. Flank, *J. Am. Chem. Soc.* **1995**, *117*, 1019.
[29] C. Hannay, M. J. Hubin-Franskin, F. Grandjean, V. Briois, J. P. Itie, A. Polian, S. Trofimenko, G. J. Long, *Inorg. Chem.* **1997**, *36*, 5580.
[30] C. Bressler, M. Chergui, *Chem. Rev.* **2004**, *104*, 1781.
[31] W. Gawelda, A. Cannizzo, V.-T. Pham, F. van Mourik, C. Bressler, M. Chergui, *J. Am. Chem. Soc*. **2007**, submitted.
[32] A. L. Ankudinov, B. Ravel, J. J. Rehr, S. D. Conradson, *Phys. Rev. B* **1998**, *58*, 7565.
[33] M. Khalil, M. A. Marcus, A. L. Smeigh, J. K. McCusker, H. H. W. Chong, R. W. Schoenlein, *J. Phys. Chem. A* **2006**, *110*, 38.
[34] A. Hauser, N. Amstutz, S. Delahaye, A. Sadki, S. Schenker, R. Sieber, M. Zerara, *Chimia* **2002**, *56*, 685.
[35] G. Ingold, R. Abela, P. Beaud, D. Grolimund, S. Johnson, M. Munoz, L. Rivkin, V. Schlott, T. Schmidt, L. Schulz, A. Streun, J. F. van der Veen, O. Chubar, S. Khan, A. Tarnovsky, *PSI Scientific Reports*, **2002**, Vol. VII.